https://doi.org/10.5194/bg-2022-171
Preprint. Discussion started: 19 August 2022
© Author(s) 2022. CC BY 4.0 License.

Biogeosciences Discussions

# Variations of carbon flux at different time scales in a semi-fixed sandy land ecosystem in Horqin Sandy Land, China

Yayi Niu[a,c,d], Yuqiang Li[a,b,c,d]*, Wei Liu[a,c], Xuyang Wang[a,c,d], Yun Chen[a,c,d]

[a] Northwest Institute of Eco-Environment and Resources, Chinese Academy of Sciences, Lanzhou 730000, China

[b] Key Laboratory of Strategic Mineral Resources of the Upper Yellow River, Ministry of Natural Resources, Lanzhou 730000, China

[c] University of Chinese Academy of Sciences, Beijing 100049, China

[d] Naiman Desertification Research Station, Northwest Institute of Eco-Environment and Resources, Chinese Academy of Sciences, Tongliao 028300, China

* *Correspondence to*: Yuqiang Li (liyq@lzb.ac.cn)

320 Donggang West Road, Lanzhou, 730000, China

Phone/Fax: 86-931-496-7219

https://doi.org/10.5194/bg-2022-171
Preprint. Discussion started: 19 August 2022
© Author(s) 2022. CC BY 4.0 License.



**Abstract**

Sandy land is an important part of terrestrial ecosystem, which has a substantial impact on maintaining global ecological health and security. However, there is still a scarcity representative studies of climate change's effect on the carbon fluxes (*NEE*: net ecosystem $CO_2$ exchange; $R_{eco}$: ecosystem respiration; *GPP*: gross primary productivity). Eddy covariance technique was used to determine carbon fluxes and climatic conditions in this ecosystem from 2017 to 2021. At an annual scale, the semi-fixed sandy land was found to be a net carbon release, the value of annual average *NEE* was 6.81 ± 36.35 g C $m^{-2}$ $yr^{-1}$. It functioned as a carbon source in dry years (2017 and 2020), but was a carbon sink in wet years (2019 and 2021) and a normal year (2018). At seasonal scale, according to the Random Forest, deep soil water content ($SWC_{80}$) and photosynthetic photon flux density had a great impact on *NEE* and *GPP*, whereas shallow and deep soil water ($SWC_{10}$ and $SWC_{80}$) dominated $R_{eco}$. At a monthly scale, the multiple stepwise regression showed that soil temperature, precipitation (*PPT*) and *SWC* were the dominant environmental factors. At an annual scale, correlation analysis showed that total annual *PPT* was negatively correlated with *NEE*. Our results illustrate the importance of climate variations for the *NEE*, $R_{eco}$, and *GPP* at different time scales in arid and semi-arid areas. They also highlight the importance of water availability (the pattern and intensity of *PPT* and *SWC* at different depths) on regional and global carbon cycles.

**Keywords:** Precipitation; Net ecosystem $CO_2$ exchange; Carbon flux; Climate change; Semi-fixed sandy land

## 1. Introduction

Human activities have led to unprecedented and devastating global climate change, including altered precipitation patterns, increased temperature and $CO_2$ concentration (IPCC, 2007; Yu et al., 2013). $CO_2$ plays a major role in Earth's mass and energy budgets, so quantifying ecosystem carbon cycles and carbon budgets is essential for planning a sustainable future (McGuire et al., 2009; Ma et al., 2020). The balance between photosynthesis (gross primary productivity (*GPP*)) and respiration (ecosystem

https://doi.org/10.5194/bg-2022-171
Preprint. Discussion started: 19 August 2022
© Author(s) 2022. CC BY 4.0 License.
Biogeosciences Discussions

respiration ($R_{eco}$)) determines the net ecosystem $CO_2$ exchange (*NEE*) in terrestrial ecosystems (Schmitt et al., 2010; Lasslop et al., 2010; Zhang et al., 2019). As a result, comprehending the dynamics processes and underlying mechanisms of *NEE* is a crucial issue in global change research (Yu et al., 2013). In particular, the division of *NEE* into *GPP* and $R_{eco}$, which depict the fundamental mechanisms, is conducive to supply a process-level, mechanistic comprehension of the regional carbon balance (Reichstein et al., 2005; Jassal et al., 2007; Lasslop et al., 2010; Cao et al., 2021).

About 30% of the earth's surface is covered by arid and semiarid areas (Kefi et al., 2008; Poulter et al., 2014). Ecosystems in these areas are at risk of soil erosion and degradation, which is resulting from a combination of climate change, such as increasing intensity and frequency of extreme climate events (eg., drought and extreme precipitation) (Knapp et al., 2015), and unreasonable human activities, including overgrazing, firewood harvesting, and excessive deforestation (Domingo et al., 2011; Wang et al., 2021). Despite the fact that many research on carbon fluxes through ecosystems in semi-arid areas have been conducted to date (Du and Liu, 2013; Hao et al., 2017; Niu et al., 2020; Zhang et al., 2020), we still don't fully understand how these ecosystems function as $CO_2$ sources or sinks (Huxman et al., 2004; Ma et al., 2007; Zhou et al., 2020; Niu et al., 2021). Therefore, further investigation is required to study the carbon budget and its controlling mechanisms for a wider range of ecosystems, particularly in drylands, to more accurately evaluate global carbon budgets.

The original landscape of China's Horqin Sandy Land was a sparse shrubland and grassland with hydrothermal conditions that are adequate to support shrubs, an abundant plant community with a diverse composition, a stable ecosystem structure, and high productivity. However, due to the disturbance caused by extensive human activities and the cultivation of a large area of land, nearly 80% of the region has experienced aeolian desertification (Liu et al., 1996; Zhao et al., 2007; Li et al., 2019; Niu et al., 2020). The region's eco-environment is extremely fragile and vulnerable to damage (Meng et al., 2008; Zhu et al., 2020). Grassland, cropland, and ecosystems with semi-fixed sands are the main land uses in this study area (Duan et al., 2019; Zhu et al., 2020). Previous researches in this area have shown that the recovering sandy grassland

https://doi.org/10.5194/bg-2022-171
Preprint. Discussion started: 19 August 2022
© Author(s) 2022. CC BY 4.0 License.

ecosystem was a carbon release, whereas the sandy maize cropland ecosystem was a carbon sink on an annual scale, and that the amount of carbon sequestration in both ecosystems increased with increasing precipitation (Niu et al., 2020, 2021). To the best of our knowledge, the carbon fluxes of this semi-fixed sandy land ecosystem in this region have received little attention (e.g., Hu et al., 2015), so more studies are needed to understand the characteristics of carbon flux at the ecosystem scale, especially for semi-fixed sandy land protected by grazing exclusion using fences to allow natural recovery. Long-term continuous monitoring of the carbon flux characteristics and the influencing factors in the semi-fixed sandy land will complement and improve our understanding of the present carbon budgets of the world's dryland ecosystems.

Studies have found that numerous meteorological factors can play a vital importance in regulating carbon flux (*NEE*, *GPP* and $R_{eco}$) (Hu et al., 2010; Papale et al., 2015; Tang et al., 2018; Zhang et al., 2018a; Watham et al., 2021). For example, previous studies have shown that photosynthetic photon flux density (*PPFD*), air and soil temperatures, precipitation (*PPT*), soil water content (*SWC*), and vapor pressure deficit (*VPD*) most strongly controlled the dynamics of ecosystem carbon fluxes (Jia et al., 2014, 2016; Liu et al., 2019). However, the availability of water is generally the main constraining factor that affects the carbon flux characteristics of the system in water-limited ecosystems (Fu et al., 2006; Zhang et al., 2019; Zhou et al., 2020; Niu et al., 2020, 2021), so water-related parameters like *PPT*, *SWC*, and *VPD* have a significant impact on the variations in carbon fluxes at different temporal scales (Noormets et al., 2010; Gao et al., 2012; Jia et al., 2014; Niu et al., 2020). Both *GPP* and $R_{\mathrm{eco}}$ may be limited by low water availability (Yuan et al., 2010; Zhou et al., 2013; Zhang et al., 2018). The depression of *GPP* results from limitations on plant physiological processes and alterations of plant phenology (Meir and Woodward, 2010; Zhou et al., 2013), whereas the depression of $R_{\mathrm{eco}}$ results from decreased root respiration (Linn and Doran, 1984; Bouma et al., 1997; Lee et al., 2003), decreased soil microorganism activity (Skopp et al., 1990; Drenovsky et al., 2004), and decreased decomposition of organic matter (Liu et al., 2009; Moyano et al., 2012; Cuevas et al., 2013; Wang et al., 2014). Therefore, quantifying how precipitation affects soil water regimes, and how these

https://doi.org/10.5194/bg-2022-171
Preprint. Discussion started: 19 August 2022
© Author(s) 2022. CC BY 4.0 License.


changes influence *NEE*, *GPP* and $R_{eco}$, is critical to evaluate the vulnerability of sandy land ecosystems to climate change, which will be important information to support development of strategies to preserve or restore these sandy lands (Zhang et al., 2019; Niu et al., 2020).

In this paper, we concentrated on carbon fluxes (*NEE*, $R_{\mathrm{eco}}$, and *GPP*) from 2017 to 2021 in a semi-fixed sandy land ecosystem in Inner Mongolia, China. Our main goals were to (1) quantify the inter-annual, seasonal, and monthly changes of carbon fluxes (*NEE*, $R_{\mathrm{eco}}$, and *GPP*); (2) identify the environmental variables that control these variations at the different time scales; and (3) given that *PPT* and *SWC* are dominant factors that influence carbon fluxes in sandy maize cropland and sandy grassland ecosystems in this region (Niu et al., 2020, 2021), identify the impact of *PPT* and *SWC* on carbon fluxes in the semi-fixed sandy land ecosystem. Our research hypothesis was that changes in climate factors at different temporal scales, and particularly changes in *PPT* and *SWC*, would affect *NEE*, *GPP*, and $R_{\mathrm{eco}}$ through both direct and indirect mechanisms.

## 2. Materials and methods

### 2.1 Site description

The research was conducted at the Horqin Sandy Land in Naiman Banner, Tongliao City, Inner Mongolia, China (42° 55′N, 120° 42′ E, 377 m a.s.l.) (Fig. 1)). The study site became severely desertified due to over reclamation and overgrazing. A series of grazing exclosures were erected in 2005 to restore the function of degraded ecosystem.

The climate features of the site are temperate continental semiarid monsoon climate, with average annual temperature was 6.8 °C, varying from −9.6 °C in January and 24.6 °C in July. The mean annual precipitation was 360 mm, a large portion of annual precipitation (70 %) occurs from May to September (Niu et al., 2020, 2021). The soil in this site are chestnut soil and Aeolian sandy soil (Zhao et al., 2007; Niu et al., 2020). Soil texture of topsoil (0-20 cm) is comprised by 92% coarse sand, 2% fine sand, and 6% clay, respectively. Other soil properties such as pH, soil organic carbon, bulk density, total nitrogen contents, and field capacity were 7.42, 2.47 g $kg^{-1}$, 1.66 g $cm^{-3}$, 0.16 g $kg^{-1}$, and 24.5%, respectively. Vegetation basal cover ranges from 30% to 60%,

https://doi.org/10.5194/bg-2022-171
Preprint. Discussion started: 19 August 2022
© Author(s) 2022. CC BY 4.0 License.


dominated by *Caragana microphylla* in the shrub layer, and the herbaceous species included *Setaria viridis*, *Pennisetum centrasiaticum*, *Chloris virgata*, and *Artemisia scoparia*.

**2.2 Carbon fluxes and micrometeorological measurements**

The eddy covariance (EC) method was utilized to determine $CO_2$ flux at half-hourly intervals from 2017 to 2021. *PPFD*, air temperature ($T_a$), precipitation (*PPT*), soil heat flux at two depths (5 and 10 cm), soil water content (*SWC*) and the soil temperature ($T_s$) at four depths (10, 30, 50, and 80 cm) were also measured. A complete description of the equipment used and protocols for eddy covariance data processing (including raw 10 Hz data, 30-min data quality and gap filling methods) are described in Niu et al. (2020; 2021). The degree of energy closure was used to assess the data quality of an EC system (Wilson et al. 2002). The energy closures ranged from 0.48 to 0.67 throughout our study (Fig. S1), indicating that the data observed at our study site met the observation requirements (Wilson et al. 2002; Niu et al., 2021).

**2.3 Random Forest and statistical analyses**

The Random Forest analysis was used to identify the main influencing factors of seasonal *NEE*, $R_{eco}$ and *GPP* among the meteorological factors (*PPT*, *PPFD*, $T_a$, *VPD*, the $T_s$ and *SWC* at four depths) (Pham and Brabyn, 2017). Because the root system of the natural *Caragana microphylla* shrubs is mainly found above a depth of 80 cm (A et al., 2003), we measured the *SWC* and $T_s$ at depths of 10, 30, 50, and 80 cm. More detailed procedures for Random Forest can found in Zhou et al. (2020) and Niu et al. (2021).

We also used multiple stepwise regression analysis to identify the key environment factors (*PPT*, *PPFD*, $T_a$, *VPD*, and the $T_s$ and *SWC* at depths of 10, 30, 50 and 80 cm) linked to monthly scale *NEE*, $R_{eco}$ and *GPP*. The higher *F*-values represent a better fit. For the data at an inter-annual scale, the relationship between the climatic factors and the carbon fluxes was determined using correlation analysis (Pearson's *r*). We used SPSS (22.0 version Inc. Chicago, IL) software to perform all descriptive statistics and statistical analyses (including multiple stepwise regression analysis, single-factor analysis of variance (ANOVA), and correlation analysis). We used least-significant-different (LSD) test to determine pairs of values that differed significantly. We used version 8.0 of the Origin software (OriginLab Corporation, Northampton, MA, USA) for graphing our results.

## 3. Results

### 3.1 Meteorological conditions

Environmental factors showed apparent seasonal variations (Fig. 2). Temperature ($T_a$ and $T_s$) and *PPFD* both followed unimodal type distribution. During the observation period, the mean annual *PPFD* was 22.14 mol m$^{-2}$ d$^{-1}$ (Table 1), with daily values ranging from 1.89 mol m$^{-2}$ d$^{-1}$ on 13 February 2020 to 48.44 mol m$^{-2}$ d$^{-1}$ on 15 June 2020. The *PPFD* was significantly lower in 2020 (1544 mol m$^{-2}$ d$^{-1}$) than in the other years, and there was no difference among the other years. The mean annual $T_a$ was 8.2 ℃ (Table 1), with daily values ranging from -23.61 ℃ on 7 January 2021 to 32.16 ℃ on 3 August 2021. The mean annual $T_{s10}$, $T_{s30}$, $T_{s50}$, and $T_{s80}$ were 9.94, 10.26, 10.63, and 10.97 ℃, respectively, with daily values of $T_{s10}$ ranging from -18.74 ℃ on 27 January 2018 to 36.04 ℃ on 26 July 2020, daily values of $T_{s30}$ ranging from -13.92 ℃ on 27 January 2018 to 36.67 ℃ on 25 July 2020, daily values of $T_{s50}$ ranging from -9.89 ℃ on 28 January 2018 to 27.61 ℃ on 16 July 2017, and daily values of $T_{s80}$ ranging from -7.97 ℃ on 25 January 2017 to 25.72 ℃ on 6 August 2018. The mean annual $T_a$ did not differ appreciably across years, but the mean annual $T_s$ did not differ significantly among the years at any depth ($P > 0.05$).

The annual cumulative *PPT* varied greatly during the observation period from 2017 to 2021, and differed significantly between many pairs of years (Fig. 2f and Table 1): it averaged 313 mm in 2017, 351 mm in 2018, 382 mm in 2019, 312 mm in 2020, and 430 mm in 2021. As a result, the *PPT* in 2017 and 2020 were less than in a typical year (long-term average of 360 mm for 1960-2014; Niu et al., 2020), whereas 2018 was near to a normal year. *SWC* followed the same general trend as *PPT* (Fig. 2e).

*VPD* is also related to *PPT*, but it has the opposite pattern as *SWC*. *VPD* showed a unimodal type (Fig. 2a). However, the mean value did not differ significantly among the years, except for a significantly higher value in the dry year 2017 (Table 1).

https://doi.org/10.5194/bg-2022-171
Preprint. Discussion started: 19 August 2022
© Author(s) 2022. CC BY 4.0 License.


### 3.2 Variations in carbon fluxes

*NEE*, $R_{eco}$, and *GPP* showed obvious seasonal changes throughout the growing season (from May to September), whereas *NEE* was generally stable across years outside the growing season (Fig. 3). Daily *NEE*, $R_{eco}$, and *GPP* showed resemble seasonal dynamics during the whole study period, and only a few days during the growing season showed net carbon emission; the rest showed carbon absorption. However, the size of *NEE*, $R_{eco}$ and *GPP* varied throughout research years.

At a monthly scale (Fig. 4a-e), $R_{eco}$ and *GPP* generally showed unimodal trends and peaked in July. An exception was the June peak in 2020, a year when *PPFD* was significantly lower than in all other years; Table 1), with lower $R_{eco}$ and *GPP* all year compared with the other years (Fig. 4d). Due to the influence of *PPT* and *SWC* on these fluxes, *NEE* in the wet years showed carbon absorption throughout the growing season (from May to August in 2019 and 2021; Fig. 4c, e; Table 1), whereas in the dry and not significantly different from the long-term average close to a normal year, *NEE* showed carbon absorption in about 3 months and carbon emission in the other months (2017, 2018 and 2020; Fig. 4a, b, d; Table 1).

At an annual scale (Fig. 4f), this study shows that the mean *NEE*, $R_{eco}$, and *GPP* were 6.81 ± 36.35, 664.78 ± 31.49, and 658.79 ± 46.11 g C $m^{-2}$ $yr^{-1}$, respectively. In the wet years (2019 and 2021), the semi-fixed sandy land showed carbon sequestration, the cumulative annual *NEE* were -14.14 and -126.14 g C $m^{-2}$ $yr^{-1}$, respectively. In contrast, in the dry years (2017 and 2020) and the normal year (2018), the system showed carbon emissions, the cumulative annual *NEE* were 48.50, 51.17, and 74.66 g C $m^{-2}$ $yr^{-1}$, respectively.

### 3.3 Relationships between meteorological factors and *NEE*, $R_{eco}$ and *GPP*

The environment factors and *NEE* were largely stable during dormant season in all years, so in the rest of this paper, we will concentrate on the relationships between the carbon fluxes and the meteorological factors during the growing season. Figure 5 illustrates the variable importance values from the Random Forest analysis, which represent the contributions of the variables to *NEE*, $R_{eco}$, and *GPP*. The goodness of fit measure of the random forest analysis is shown in Fig. S2. For *NEE*, the most critical

https://doi.org/10.5194/bg-2022-171
Preprint. Discussion started: 19 August 2022
© Author(s) 2022. CC BY 4.0 License.


variable was *PPFD*, with an importance of 68.6%, followed by the factors associated with moisture (44.4% for $SWC_{80}$, 39.3% for *PPT*, 36.7% for $SWC_{30}$, 34.8% for $SWC_{50}$, *VPD* for 34.0%, and 27.1% for $SWC_{10}$), which were all significant at $P < 0.01$. For $R_{eco}$, the soil shallow *SWC* ($SWC_{10}$) and deep *SWC* ($SWC_{80}$) were the most important variables, with importance values of 73.4% and 65.1%, respectively, followed by temperature (61.2% for $T_a$ and 46.9% for $T_{s50}$), $SWC_{30}$ (41.0%), and *PPFD* (27.63%), which were all significant at $P < 0.01$ (except for $SWC_{30}$, which was significant at $P < 0.05$). For *GPP*, *PPFD* was the most important factor, with an importance of 67.48%, followed by the factors associated with moisture (55.3% for $SWC_{80}$, 50.7% for $SWC_{50}$, and 44.6% for $SWC_{30}$, and 48.3% for $SWC_{10}$). These were followed by two temperature variables ($T_{s50}$ and $T_a$ and 44.0% and 36.7%), which were significant at $P < 0.01$. In general, *PPFD*, deep soil moisture ($SWC_{80}$) and shallow soil moisture ($SWC_{30}$ and $SWC_{10}$) were the main environmental factors that affected all three carbon fluxes at a seasonal scale, and they showed a strong and negative relationship with *NEE* and a significant positive relationship with $R_{eco}$ and *GPP* (Fig. 6); that is, the ecosystem's carbon sequestration potential rose as *PPFD* and *SWC* increased.

We used the multiple regression analysis to reveal the relationships between the *NEE*, $R_{eco}$, and *GPP* and environmental parameters to determine the main influencing factors that resulted in the monthly variation in carbon fluxes. The results are summarized in Table 2. We found that 65% of the *NEE* variation could be explained by a combination of $T_{s50}$, $SWC_{30}$, *VPD*, and *PPFD* ($F$=28.75, $R^2$=0.65, $P < 0.001$). We found that 83% of the variations of $R_{eco}$ could be explained by a combination of $T_{s10}$, *PPT*, and $SWC_{10}$ ($F$=91.96, $R^2$=0.83, $P < 0.001$). Similarly, 85% of the variations of *GPP* could be described by a combination of $T_{s10}$, *PPT*, $SWC_{80}$, and $SWC_{10}$ ($F$=82.62, $R^2$=0.85, $P < 0.001$). Generally, $T_{s10}$, *PPT*, and *SWC* explained a large amount of the carbon flux variations. The correlations between the key variables and the carbon fluxes were highest for $T_{s10}$, *PPT*, and *SWC* in each model (Figs. 7-9).

At the yearly scale, the mean *PPFD*, $T_a$, $T_s$ at all depths, and *VPD* were relatively stable across the study period, and the relationships between these environment factors and the *NEE*, $R_{eco}$, and *GPP* were not significant. The main environmental variation

https://doi.org/10.5194/bg-2022-171
Preprint. Discussion started: 19 August 2022
© Author(s) 2022. CC BY 4.0 License.



during the study period was the availability of water, such as *PPT* and the *SWC* at all depths (Fig. 2, Table 1). We found that *NEE* strong and negative related with *PPT*, but not related with the other environmental factors (Table 3); $R_{eco}$ didn't have a significant relationship with environmental conditions, and *GPP* was significantly positively related with *PPFD* and $SWC_{80}$. That is, the ecosystem's carbon sequestration capacity rose when *PPT*, *PPFD*, and $SWC_{80}$ increased.

## 4. Discussion

### 4.1 Comparison with other dryland ecosystems

The ecosystem of *NEE* changes largely from carbon sequestration to carbon emissions, and these changes generally rely on water availability in dryland ecosystems (Mielnick et al., 2005; Liu et al., 2012). Our study showed that the system in semi-fixed sandy land was a net carbon emission in dry years, and a weak carbon absorption in relatively wet years. The yearly mean NEE was 6.81 g C $m^{-2}$ $yr^{-1}$ during the observation period (Fig. 4f; Tables 1 and 3). Our results agree with previous findings in dryland ecosystems, which showed that the variability in *PPT* had significant influences on the carbon fixation of the *Caragana microphylla* shrub-dominated ecosystem, leading it to alternate rapidly between carbon sequestration and carbon emission (Jia et al., 2016; Liu et al., 2016). However, the magnitude of the average annual *NEE* in the current study was lower than those in a mixture of xerophytic shrub species (the mean *NEE* was -77 g C $m^{-2}$ $yr^{-1}$ ); in a phreatophyte-dominated in China's Gurbantünggüt Desert ecosystem, where the *NEE* ranged from -40 to -5 g C $m^{-2}$ $yr^{-1}$ (Liu et al., 2016); in a *Lycium andersonii* and *Ambrosia dumosa* shrubland ecosystem, where the *NEE* was -127 g C $m^{-2}$ $yr^{-1}$ (Jasoni et al., 2005); and in a mature semi-arid shrub ecosystem in California (USA) dominated by *Adenostoma fasciculatum*, where *NEE* ranged from -155 to -96 g C $m^{-2}$ $yr^{-1}$ (Luo et al., 2007). However, the carbon sequestration capacity of the semi-fixed sandy land ecosystem was higher than that of a recovering sandy grassland in our study region that was dominated by herbaceous species (the average annual of *NEE* was 49 g C $m^{-2}$ $yr^{-1}$ from 2015-2018) (Niu et al., 2020). The most plausible explanation for the difference between the two areas relates to differences in the vegetation types. Zhang (2007) demonstrated that the carbon fixation capacity of

https://doi.org/10.5194/bg-2022-171
Preprint. Discussion started: 19 August 2022
© Author(s) 2022. CC BY 4.0 License.



*Caragana microphylla* was higher than that of herbaceous and sub-shrub plants such as *Artemisia frigida* in Horqin Sandy Land.

**4.2 Impacts of environmental condition on carbon fluxes**

Carbon fluxes are influenced by a variety of environmental factors in complicated and interacting ways, and the main control factors change substantially across time scales (Fu et al., 2009; Niu et al., 2010; Zhang et al., 2018a). At a seasonal scale, our Random Forest results showed that *PPFD* and deep *SWC* ($SWC_{80}$) were the most important environmental drivers for *GPP* and *NEE* (Fig. 5), which were both significantly negatively related with *GPP* and strong positively related with *NEE* (Fig. 6), suggesting that light and soil water stress were limiting photosynthetic activity. As the main energy source for plant photosynthesis, *PPFD* plays an important role in plant carbon fixation, so with increasing *PPFD*, an ecosystem's carbon sequestration capacity generally increases (Zhou et al., 2020; Niu et al., 2021). Our results also demonstrated that deep *SWC* ($SWC_{80}$) affected the seasonal variation of *NEE* and *GPP* (Fig. 5, 6), since the deep *SWC* would be closely linked to large precipitation pulses; for example, $PPT > 20$ mm caused synchronous increases in $SWC_{80}$ in our study (Fig. S3). This is because the larger amount of precipitation can infiltrate into the soil and replenish the deep soil moisture, where it becomes plant-available and can sustain net photosynthesis (Niu et al., 2020). This result was also similar with previous studies in dryland ecosystems (Austin et al., 2004; Kurc and Small, 2007; Tang et al., 2018). For seasonal $R_{eco}$, shallow *SWC* ($SWC_{10}$) was the most important factor, followed by deep *SWC* ($SWC_{80}$) (Fig. 5, 6). Smaller rainfall events ($PPT < 20$ mm; Fig. S3) may alter the shallow *SWC* and increase shallow soil microbial respiration (Thomey et al. 2011); the duration and extent of the microbial metabolic reaction appear to be tightly linked with the availability of shallow soil water content (Huxman et al., 2004). In addition, large rainfall pulses ($PPT > 20$ mm; Fig. S3) trigger plant root activity in deeper soil layers (Potts et al., 2006). These findings suggest that precipitation mainly affects carbon fluxes (*NEE*, $R_{eco}$, and *GPP*) at a seasonal scale by affecting *SWC* in different soil layers in our research system.

https://doi.org/10.5194/bg-2022-171
Preprint. Discussion started: 19 August 2022
© Author(s) 2022. CC BY 4.0 License.


At a monthly scale, soil temperature was an essential factor that determined the carbon fluxes, followed by water-related factors such as the monthly total *PPT* and $SWC_{30}$, $SWC_{80}$, and $SWC_{10}$ (Table 3; Figs. 7-9). $T_s$ and *SWC* are often regarded as the primary regulators of ecosystem respiration (Helbling et al., 2003; Kelsey et al., 2011; Zhang et al., 2018b; Chang et al., 2021), and our results are consistent with this view. $R_{eco}$ increased with increasing shallow soil temperature ($T_{s10}$), monthly total *PPT*, and shallow *SWC* ($SWC_{10}$) (Fig. 8). The increase was exponential between $R_{eco}$ and $T_{s10}$ (Fig. 8a), which is most likely explained by the influence of soil temperature on microbial activity, root respiration, and soil enzyme decomposition (Jassal et al., 2008; Wang et al., 2014). $R_{eco}$ increased significantly with linear increases in the moisture-related factors (*PPT* and $SWC_{10}$) (Fig. 8b, c). This may be because root activity regulates the decomposition of soil organic matter and its influence on the microbial community can limit or increase $R_{eco}$ (Moyano et al., 2012; Wang et al., 2014).

*GPP* also increased with increasing $T_{s10}$, total *PPT*, $SWC_{80}$ and $SWC_{10}$ at monthly scale (Fig. 9). $T_s$ is one of the most important environmental influences on the formation and function of the photosynthetic apparatus (Georgieva and Yordanov, 1993; Huxman et al., 2004; Lin et al., 2005). Water is also the main variable influencing plant productivity and the carbon cycle in water-limited ecosystems, plant may rise their photosynthetic rates in reaction to *PPT* by increasing leaf-level $CO_2$ exchange, adding more leaf area incrementally, or through a combination of both responses (Liu et al., 2012; Hao et al., 2013; Niu et al., 2020, 2021). *PPT* events may influence *GPP* and $R_{eco}$ differently, thus changing the balance between them and changing the monthly *NEE* (Hao et al., 2013). Our studies are similar to previous research: *GPP* was more sensitive than $R_{eco}$ to *PPT* (Figs. 8b, 9b); the slope of the response was higher for *GPP* (1.33) than for $R_{eco}$ (0.92) in this area of the sandy grassland and in a sandy maize cropland ecosystem (Niu et al., 2020, 2021).

At the annual timescale, *PPT* was the preponderate factor that regulated the annual *NEE* in our semi-fixed sandy land. *NEE* was significantly negatively correlated to *PPT* on an annual basis during the study period (Table 3). Most previous studies showed that the magnitude and number of *PPT* incidents are important factors in regional climate

https://doi.org/10.5194/bg-2022-171
Preprint. Discussion started: 19 August 2022
© Author(s) 2022. CC BY 4.0 License.

change, as these factors can convert biological processes at an ecosystem level (Hao et al., 2013; Liu et al., 2012). The total *PPT* and related changes of *SWC* perform the most important part in drylands through their impact on plant photosynthesis by altering stomatal conductance and leaf area (Harper et al., 2005; Ford et al., 2008; Niu et al., 2020). However, they also alter ecosystem respiration processes by affecting substrate availability of soil microbial respiration (Epstein et al., 1997; Hao et al., 2013; Shi et al., 2014; Niu et al., 2020).

In summary, the three carbon fluxes (*NEE*, $R_{eco}$, and *GPP*) are not affected by single factors, but rather by a combination of a variety of environment parameters. However, when the time scale gets longer, the important factors affecting the changes of *NEE*, $R_{eco}$, and *GPP* preferred to converge. At the daily timescale, their values were influenced by radiation, temperature, and water, but at the monthly and annual timescale, the primary governing factor varied to water. Generally, water performed a key role in the change of ecosystem carbon fluxes at all the time scale.

## 5. Conclusion

We studied the carbon fluxes and their environmental driving factors at different time scales in a semi-fixed sandy land. Our results indicated that the carbon source or sink intensity of the ecosystem, which is undergoing restoration to combat desertification in the Horqin Sandy Land, and it's consistent with our hypothesis, is greatly uncertain due to the complex and interacting influences of environmental factors, especially for precipitation. In the wet years (2019 and 2021), the semi-fixed sandy land was a carbon sink, whereas in the dry years (2017 and 2020) and the normal year (2018), the system showed a carbon source, with a mean annual *NEE* of 6.81 g C $m^{-2}$ $yr^{-1}$.

We determined the primary governing factors of *NEE*, $R_{eco}$, and *GPP* using correlation analyses, Random Forest models, and multiple stepwise regression analysis. *PPFD* and deep *SWC* ($SWC_{80}$) were important drivers for the seasonal variation of *NEE* and *GPP*, whereas both shallow and deep *SWC* ($SWC_{10}$ and $SWC_{80}$) were important drivers for $R_{eco}$. At a monthly scale, $T_s$, *PPT*, and $SWC_{10}$ were strong positively related to $R_{eco}$ and *GPP*, whereas *NEE* was strong negatively related to $T_{s50}$, *PPT*, and $SWC_{30}$. Annual *NEE* was strongly correlated with the total *PPT*. Water performed a key role in

https://doi.org/10.5194/bg-2022-171
Preprint. Discussion started: 19 August 2022
© Author(s) 2022. CC BY 4.0 License.


the changes of ecosystem carbon fluxes in our semi-fixed sandy land ecosystem. If regional precipitation increases in the future, the potential carbon sequestration in semi-fixed sandy land ecosystem is likely to increase.

## Data Availability

In agreement with the FAIR Data standards, the data used in this article are archived, published, and available in a dedicated repository: https://doi.org/10.4121/20071877.

## Author contributions

YQL, YYN, WL, XYW, and YC designed the study, YYN analyzed the data. YYN drafted the manuscript. All co-authors had a chance to review the manuscript and contributed to discussion and interpretation of the data.

## Competing interests

The authors declare that they have no known competing financial interests or personal relationships that could have appeared to influence the work reported in this paper.

## Acknowledgments

This research was supported by the National Natural Science Foundation of China (grants 31971466 and 32001214) and the National Key Research and Development Program of China (2017YFA0604803 and 2017YFA0604801).

## References

A, L. M. S., Jiang, D. M., Pei, T. F.: Relationship between root system distribution and soil moisture of artificial *Caragana microphylla* vegetation in Sandy Land (in Chinese), J. Soil Water 17, 79-81, https://doi.org/10.13870/j.cnki.stbcxb.2003.03.022, 2003.

Austin, A. T., Yahdjian, L., Stark, J. M., Belnap, J., Porporato, A., Norton, U., Schaeffer, S. M.: Water pulses and biogeochemical cycles in arid and semiarid ecosystems, Oecologia, 141, 221–235, https://doi.org/10.1007/s00442-004-1519-1, 2004.

Bouma, T. J., Kai, L. N., Eissenstat, D. M., Lynch, J. P.: Estimating respiration of roots in soil: interactions with soil $CO_2$, soil temperature and soil water content, Plant Soil, 195, 221-232, https://doi.org/10.1023/A:1004278421334, 1997.

Cao, D., Zhang, J. H., Xun, L., Yang, S. S., Yao, F. M.: Spatiotemporal variations of global terrestrial vegetation climate potential productivity under climate change.

https://doi.org/10.5194/bg-2022-171
Preprint. Discussion started: 19 August 2022
© Author(s) 2022. CC BY 4.0 License.

Sci. Total Environ., 145320, https://doi.org/10.1016/j.scitotenv.2021.145320, 2021.

Chang, Y., Zhang, R., Hai, C., Zhang, L.: Seasonal variation in soil temperature and moisture of a desert steppe environment: a case study from Xilamuren, Inner Mongolia, Environ. Earth Sci., 80, 1-12, https://doi.org/10.1007/s12665-021-09393-0, 2021.

Cuevas, R. M., Hidalgo, C., Payán, F., Etchevers, J. D., Campo, J.: Precipitation influences on active fractions of soil organic matter in seasonally dry tropical forests of the Yucatan: regional and seasonal patterns, Eur. J. Forest. Res., 132(5), 667-677, https://doi.org/10.1007/s10342-013-0703-4, 2013.

Domingo, F., Serrano-Ortiz, P., Were, A., Villagarcia, L., Garcia, M., Ramirez. D.A., Kowalski, A. S., Moro, M. J., Rey, A., Oyonarte, C.: Carbon and water exchange in semiarid ecosystems in SE Spain. J. Arid Environ., 75, 1271-1281, https://doi.org/10.1016/j.jaridenv.2011.06.018, 2011.

Drenovsky, R. E., Vo, D., Graham, K. J., Scow, K. M.: Soil water content and organic carbon availability are major determinants of soil microbial community composition, Microb. Ecol., 48, 424-430, https://doi.org/10.1007/s00248-003-1063-2, 2004

Du, Q., Liu, H. Z.: Seven years of carbon dioxide exchange over a degraded grassland and a cropland with maize ecosystems in a semiarid area of China, Agric. Ecosyst. Environ., 173, 1-12, https://doi.org/10.1016/j.agee.2013.04.009, 2013.

Duan, H. C., Wang, T., Xue, X., Yan, C. Z.: Dynamic monitoring of aeolian desertification based on multiple indicators in Horqin Sandy Land, China, Sci. Total Environ., 650, 2374-2388, https://doi.org/10.1016/j.scitotenv.2018.09.374, 2019.

Epstein, H. E., Lauenroth, W. K., Burke, I. C.: Effects of temperature and soil texture on ANPP in the U.S. Great Plains, Ecology, 78, 2628–2631, https://doi.org/10.2307/2265921, 1997.

https://doi.org/10.5194/bg-2022-171
Preprint. Discussion started: 19 August 2022
© Author(s) 2022. CC BY 4.0 License.

Biogeosciences
Discussions

Ford, C. R., Mitchell, R. J., Teskey, R. O.: Water table depth affects productivity, water use, and the response to nitrogen addition in a savanna system, Can. J. For. Res., 38, 2118–2127, https://doi.org/10.1139/X08-061, 2008.

Fu, Y. L., Yu, G. R., Sun, X. M., Li, Y. N., Wen, X. F., Zhang, L. M., Li, Z. Q., Zhao, L., Hao, Y. B.: Depression of net ecosystem $CO_2$ exchange in semi-arid *Leymus chinensis* steppe and alpine shrub, Agric. For. Meteorol., 137, 234-244, https://doi.org/10.1016/j.agrformet.2006.02.009, 2006.

Fu, Y. L., Zhen, Z. M., Yu, G. R., Hu, Z. M., Sun, X. M., Shi, P. L., Wang, Y. Z., Zhao, X. Q.: Environmental controls on carbon fluxes over three grassland ecosystems in China, Biogeosci. Discuss., 6, 8007-8040, https://doi.org 10.5194/bgd-6-8007-2009, 2009.

Gao, Y. H., Li, X. R., Liu, L. C., Jia, R. L., Yang, H. T., Li, G., Wei, Y. P.: Seasonal variation of carbon exchange from a revegetation area in a Chinese desert, Agric. For. Meteorol., 156, 134-142, https://doi.org/10.1016/j.agrformet.2012.01.007, 2012.

Georgieva, K., Yordanov, I.: Temperature dependence of chlorophyll fluorescence parameters of pea seedlings, J. Plant Physiol., 142, 151-155, https://doi.org/10.1016/S0176-1617(11)80955-7, 1993.

Hao, Y. B., Kang, X. M., Wu, X., Cui, X. Y., Liu, W. J., Zhang, H., Li, Y., Wang, Y. F., Xu, Z. Z., Zhao, H. T.: Is frequency or amount of precipitation more important in controlling $CO_2$ fluxes in the 30-year-old fenced and the moderately grazed temperate steppe? Agric. Ecosyst. Environ., 171, 63-71, https://doi.org/10.1016/j.agee.2013.03.011, 2013.

Hao, Y. B., Zhou, C. T., Liu, W. J., Li, L. F., Kang, X. M., Jiang, L. L., Cui, X. Y., Wang, Y. F., Zhou, X. Q., Xue, C. Y. : Aboveground net primary productivity and carbon balance remain stable under extreme precipitation events in a semiarid steppe ecosystem, Agric. For. Meteorol., 240–241, 1-9, https://doi.org/10.1016/j.agrformet.2017.03.006, 2017.

Harper, C. W., Blair, J. M., Fay, P. A., Knapp, A. K., Carlisle, J. D. Increased rainfall variability and reduced rainfall amount decreases soil $CO_2$ flux in a grassland

https://doi.org/10.5194/bg-2022-171
Preprint. Discussion started: 19 August 2022
© Author(s) 2022. CC BY 4.0 License.
Biogeosciences
Discussions

ecosystem, Glob. Change Biol., 11, 322–334, https://doi.org/10.1111/j.1365-2486.2005.00899.x, 2005.

Helbling, E. W., Zagarese, H., Wetzel, R. G.: Solar radiation as an ecosystem modulator. p. 3-18 In: Helbling, E.W., Zagarese, H. (eds.) UV Effects in Aquatic Organisms and Ecosystems. Cambridge, U.K.: Royal Society of Chemistry, https://doi.org/10.1039/9781847552266-00003, 2003.

Hu, F. L., Shou, W. K., Liu, B., Liu, Z. M., Busso, C. A: Species composition and diversity, and carbon stock in a dune ecosystem in the Horqin Sandy Land of northern China, J. Arid Land. 7, 82-93, https://doi.org/10.1007/s40333-014-0038-0, 2015.

Hu, Z. M., Yu, G. R., Fu, Y. L., Sun, X. M., Li, Y. N., Chen, S. P., Wang, Y. F., Zheng, Z. M.: Effects of vegetation control on ecosystem water use efficiency within and among four grassland ecosystems in China, Glob. Change Biol., 14, 1609-1619, https://doi.org/10.1111/j.1365-2486.2008.01582.x, 2010.

Huxman, T. E., Snyder, K. A., Tissue, D., Leffler, A. J., Ogle, K., Pockman, W. T., Sandquist, D. R., Potts, D. L., Schwinning, S.: Precipitation pulses and carbon fluxes in semiarid and arid ecosystems, Oecologia, 141, 254-268, https://doi.org/10.2307/40005685, 2004.

IPCC (Intergovernmental Panel on Climate Change). Climate Change 2007: The Physical Science Basis. Summary for Policymakers. Cambridge University Press, New York (19 August 2008; http://www.ipcc.ch/ipccreports/ar4-wg1.htm), 2007.

Jasoni, R. L., Smith, S. D., Arnone, J. A. Net ecosystem $CO_2$ exchange in Mojave Desert shrublands during the eighth year of exposure to elevated $CO_2$, Glob. Change Biol., 11, 749–756, https://doi.org/10.1111/j.1365-2486.2005.00948.x, 2005.

Jassal, R. S., Black, T. A., Novak, M. D., Gaumont-Guay, D., Nesic, Z.: Effect of soil water stress on soil respiration and its temperature sensitivity in an 18-year-old temperate Douglas-fir stand, Glob. Change Biol., 14, 1305–1318, https://doi.org/10.1111/j.1365-2486.2008.01573.x, 2008.

Jassal, R. S., Black, T. A., Cai, T., Kai, M., Zhong, L., Gaumont-Guay, D., Nesic, Z.: Components of ecosystem respiration and an estimate of net primary productivity

https://doi.org/10.5194/bg-2022-171
Preprint. Discussion started: 19 August 2022
© Author(s) 2022. CC BY 4.0 License.
Biogeosciences Discussions

of an intermediate-aged douglas-fir stand, Agric. For. Meteorol., 144, 44-57, https://doi.org/10.1016/j.agrformet.2007.01.011, 2007.

Jia, X., Zha, T, Gong, J. N., Wu, B., Zhang, Y. Q., Qin, S. G.: Carbon and water exchange over a temperate semi-arid shrubland during three years of contrasting precipitation and soil moisture patterns, Agric. For. Meteorol., 228–229, 120-129, http://dx.doi.org/10.1016/j.agrformet.2016.07.007, 2016.

Jia, X., Zha, T. S., Wu, B., Zhang, Y. Q., Gong, J. N.: Biophysical controls on net ecosystem $CO_2$ exchange over a semiarid shrubland in northwest China, Biogeosciences, 11, 57-70, http://www.biogeosciences-discuss.net/11/C1064/2014/, 2014.

Kefi, S., Rietkerk, M., Katul, G. G.: Vegetation pattern shift as a result of rising atmospheric $CO_2$ in arid ecosystems, Theor. Popul. Biol., 74, 332-344, https://doi.org/10.1016/j.tpb.2008.09.004, 2008.

Kelsey, K., Wickland, K. P., Striegl, R. G.: Temperature sensitivity of boreal soil respiration across a soil moisture gradient, AGU. Fall. Meeting Abstracts, 2011.

Knapp, A. K., Hoover, D. L., Wilcox, K. R., Avolio, M. L., Koerner, S. E., La Pierre, K. J., Loik, M. E., Luo, Y., Sala, O. E., Smith, M. D.: Characterizing differences in precipitation regimes of extreme wet and dry years: implications for climate change experiments. Glob. Change Biol. 21, 2624–2633, https://doi.org/10.1111/gcb.12888, 2015.

Kurc, S. A., Small, E. E.: Soil moisture variations and ecosystem-scale fluxes of water and carbon in semiarid grassland and shrubland, Water Resour. Res., 43, 1-13, https://doi. org/10.1029/2006wr005011, 2007.

Lasslop, G., Reichstein, M., Papale, D., Richardson, A. D., Arneth, A., Barr, A., Stoy, P., Wohlfahrt, G.: Separation of net ecosystem exchange into assimilation and respiration using a light response curve approach: critical issues and global evaluation, Glob. Change Biol., 16, 187-208, http://dx.doi.org/10.1111/j.1365-2486.2009.02041.x, 2010.

Lee, M. S., Nakane, K., Nakatsubo, T., Koizumi, H. Seasonal changes in the contribution of root respiration to total soil respiration in a cool-temperate

https://doi.org/10.5194/bg-2022-171
Preprint. Discussion started: 19 August 2022
© Author(s) 2022. CC BY 4.0 License.


deciduous forest, Plant Soil., 255(1), 311-318, https://doi.org/10.1023/A:1026192607512, 2003.

Li, Y. Q., Wang, X. Y., Chen, Y. P., Luo, Y. Q., Lian, J., Niu, Y. Y., Gong, X. W., Yang, H., Yu, P. D.: Changes in surface soil organic carbon in semiarid degraded Horqin Grassland of northeastern China between the 1980s and the 2010s, Catena, 174, 217–226, https://doi.org/10.1016/j.catena.2018.11.021, 2019.

Lin, Z., Peng, C., Xu, X., Lin, G., Zhang, J. Thermostability of photosynthesis in two new chlorophyll b-less rice mutants, Science in China., 48, 139-147, https://doi.org/10.1007/BF02879666, 2005.

Linn, D. M., Doran, J. W.: Effect of water-filled pore space on carbon dioxide and nitrous oxide production in tilled and nontilled soils. Soil Sci. Soc. Am. J. 48, 1267-1272. https://doi.org/10.2136/sssaj1984.03615995004800060013x,1984.

Liu, P., Zha, T. S., Jia, X., Black, T. A., Jassal, R. S., Ma, J. Y., Bai, Y. J., Wu, Y. J. Different effects of spring and summer droughts on ecosystem carbon and water exchanges in a semiarid shrubland ecosystem in northwest China. Ecosystems, 22, 1869–1885, https://doi.org/10.1007/s10021-019-00379-5, 2019.

Liu, R., Cieraad, E., Li, Y., Ma, J. J. E. Precipitation pattern determines the inter-annual variation of herbaceous layer and carbon fluxes in a phreatophyte-dominated desert ecosystem, Ecosystems, 19, 601-614, https://doi.org/10.1007/s10021-015-9954-x, 2016.

Liu, R., Pan, L. P., Jenerette, G. D., Wang, Q. X., Cieraad, E., Yan, L. High efficiency in water use and carbon gain in a wet year for a desert halophyte community, Agric. For. Meteorol., 162–163, 127-135, https://doi.org/10.1016/j.agrformet.2012.04.015, 2012.

Liu, W. X., Zhang, Z., Wan, S. Q.: Predominant role of water in regulating soil and microbial respiration and their responses to climate change in a semiarid grassland. Glob, Change Biol., 15, 184-195, https://doi.org/10.1111/j.1365-2486.2008.01728.x, 2009

https://doi.org/10.5194/bg-2022-171
Preprint. Discussion started: 19 August 2022
© Author(s) 2022. CC BY 4.0 License.


Liu, X. M., Zhao, H. L., Zhao, A. F.: Characteristics of Sandy Environment and Vegetation in the Horqin Sandy Land. Science Press, Beijing, China (in Chinese), 1996.

Luo, H., Oechel, W. C., Hastings, S. J., Zulueta, R., Qian, Y., Kwon, H.: Mature semiarid chaparral ecosystems can be a significant sink for atmospheric carbon dioxide, Glob. Change Biol., 12, 386-396, https://doi.org/10.1111/j.1365-2486.2006.01299.x, 2007.

Ma, J., Liu, R., Li, C. H., Fan, L. L., Xu, G. Q., Li, Y.: Herbaceous layer determines the relationship between soil respiration and photosynthesis in a shrub-dominated desert plant community, Plant Soil., 449, 193-207, https://doi.org/10.1007/s11104-020-04484-6, 2020.

Ma, S., Baldocchi, D. D., Xu, L., Hehn, T.: Inter-annual variability in carbon dioxide exchange of an oak/grass savanna and open grassland in California, Agric. For. Meteorol., 147, 157-171, https://doi.org/10.1016/j.agrformet.2007.07.008, 2007.

McGuire, A. D., Euskirchen, E. S, Ruess, R. W., Kielland, K., Mcfarland, J. The changing global carbon cycle: linking plant-soil carbon dynamics to global consequences. J. Ecol. 97, 840-850, https://doi.org/10.1111/j.1365-2745.2009.01529.x, 2009.

Meir, P., Woodward, F. I.: Amazonian rain forests and drought: response and vulnerability, New Phytol., 187, 553-557, https://doi.org/ 10.2307/40792401, 2010.

Meng, Q. T., Li, Y. L., Zhao, X. Y., Zhao, Y. P., Luo, Y. Y.: Study on $CO_2$ release of leaf litters in different environment conditions in the Horqin Sandy Land (in Chinese), Arid Zone Research, 25, 519-524, https://doi.org/10.3724/SP.J.1148.2008.00259, 2008.

Mielnick, P., Dugas, W. A., Mitchell, K., Havstad, K.: Long-term measurements of $CO_2$ flux and evapotranspiration in a Chihuahuan desert grassland, J. Arid Environ., 60, 423–436, https://doi.org/10.1016/j.jaridenv.2004.06.001, 2005.

Moyano, F. E., Vasilyeva, N., Bouckaert, L., Cook, F., Craine, J., Curiel Yuste, J., Don, A., Epron, D., Formanek, P., Franzluebbers, A., Ilstedt, U., Kätterer, T., Orchard, V., Reichstein, M., Rey, A., Ruamps, L., Subke, J.A., Thomsen, I.K., Chenu, C.:

https://doi.org/10.5194/bg-2022-171
Preprint. Discussion started: 19 August 2022
© Author(s) 2022. CC BY 4.0 License.


The moisture response of soil heterotrophic respiration: interaction with soil properties, Biogeosciences, 9, 1173–1182, https://doi.org/10.5194/bg-9-1173-2012, 2012.

Niu, S. L., Wu, M. Y., Yi, H., Xia, J. Y., Li, L. H., Wan, S. Q.: Water-mediated responses of ecosystem carbon fluxes to climatic change in a temperate steppe, New Phytol. 177, 209-219, https://doi.org/10.1111/j.1469-8137.2007.02237.x, 2010.

Niu, Y. Y., Li, Y. Q., Wang, M. M., Wang, X. Y., Chen, Y.: Variations in seasonal and inter-annual carbon fluxes in a semiarid sandy maize cropland ecosystem in China's Horqin Sandy Land. Environ. Sci. Pollut. Res. 29, 5295-5312. https://doi.org/10.1007/s11356-021-15751-z, 2021.

Niu, Y. Y., Li, Y. Q., Yun, H. B., Wang, X. Y., Liu, J. Variations in diurnal and seasonal net ecosystem carbon dioxide exchange in a semiarid sandy grassland ecosystem in China's Horqin Sandy Land, Biogeosciences, 17, 6309-6326, https://doi.org/10.5194/bg-17-6309-2020, 2020.

Noormets, A., Gavazzi, M. J., Mcnulty, S. G., Domec, J. C, Sun, G. E., King, J. S., Chen, J. Q.: Response of carbon fluxes to drought in a coastal plain loblolly pine forest, Glob. Change Biol., 16, 272-287, https://doi.org/10.1111/j.1365-2486.2009.01928.x, 2010.

Papale, D., Black, T. A., Carvalhais, N., Cescatti, A., Chen, J., Jung, M., Kiely, G., Lasslop, G., Mahecha, M. D., Margolis, H. Effect of spatial sampling from European flux towers for estimating carbon and water fluxes with artificial neural networks, J. Geophys. Res-Biogeo., 120, 1941-1957, https://doi.org/10.1002/2015JG002997, 2015.

Pham, L. T. H., Brabyn, L.: Monitoring mangrove biomass change in Vietnam using SPOT images and an object-based approach combined with machine learning algorithms, ISPRS J. Photogramm Rem. Sens., 128, 86–97, https://doi.org/10.1016/j.isprsjprs.2017.03.013, 2017.

Potts, D. L., Huxman, T. E., Cable, J. M., English, N. B., Ignace, D. D., Eilts, J. A., Mason, M. J., Weltzin, J. F., Williams, D. G. Antecedent moisture and seasonal precipitation influence the response of canopy scale carbon and water exchange to

https://doi.org/10.5194/bg-2022-171
Preprint. Discussion started: 19 August 2022
© Author(s) 2022. CC BY 4.0 License.


rainfall pulses in a semiarid grassland, New Phytol, 170, 849–860, https://doi.org/10.1111/j.1469-8137.2006.01732.x, 2006.

Poulter, B., Frank, D., Ciais, P., Myneni, R. B., Andela, N., Bi, J., Broquet, G., Canadell, J. G., Chevallier, F., Liu, Y. Y.: Contribution of semi-arid ecosystems to interannual variability of the global carbon cycle, Nature, 509, 600–603, https://doi.org/10.1038/nature13376, 2014.

Reichstein, M., Falge, E., Baldocchi, D., Papale, D., Aubinet, M., Berbigier, P., Bernhofer, C., Buchmann, N., Gilmanov, T., Granier, A.: On the separation of net ecosystem exchange into assimilation and ecosystem respiration: review and improved algorithm, Glob. Change Biol., 11, 1424-1439, https://doi.org/10.1111/j.1365-2486.2005.001002.x, 2005.

Schmitt, M., Bahn, M., Wohlfahrt, G., Tappeiner, U., Cernusca, A.: Land use affects the net ecosystem $CO_2$ exchange and its components in mountain grasslands, Biogeosciences, 7, 2297, https://doi.org/10.5194/bg-7-2297-2010, 2010.

Shi, Z., Thomey, M. L., Mowll, W., Litvak, M., Brunsell, N. A., Collins, S. L., Pockman, W. T., Smith, M. D., Knapp, A. K., Luo, Y.: Differential effects of extreme drought on production and respiration: synthesis and modeling analysis, Biogeosciences, 11, 621–633, https://doi.org/10.5194/bg-11-621-2014, 2014.

Skopp, J., Jawson, M., Doran, J. W.: Steady-state aerobic microbial activity as a function of soil water content, Soil Sci. Soc. Am. J., 54, 1619-1625, https://doi.org/10.2136/sssaj1990.03615995005400060018x, 1990.

Tang, Y. K., Jiang, J., Chen, C., Chen, Y. M., Wu, X.: Rainfall pulse response of carbon fluxes in a temperate grass ecosystem in the semiarid Loess Plateau, Ecol. Evol., 8, 1-11, https://doi.org/10.1002/ece3.4587, 2018.

Thomey, M. L., Collins, S. L., Vargas, R., Johnson, J. E., Brown, R. F., Natvig, D. O., Friggens, M. T.: Effect of precipitation variability on net primary production and soil respiration in a Chihuahuan Desert grassland, Glob. Change Biol., 17, 1505–1515, https://doi.org/10.1111/j.1365-2486.2010.02363.x, 2011.

Wang, B., Zha, T. S., Jia, X., Wu, B., Zhang, Y. Q., Qin, S. G.: Soil moisture modifies the response of soil respiration to temperature in a desert shrub ecosystem,

https://doi.org/10.5194/bg-2022-171
Preprint. Discussion started: 19 August 2022
© Author(s) 2022. CC BY 4.0 License.



Biogeosci. Discuss., 10, 9213-9242, https://doi.org/10.5194/bg-11-259-2014, 2014.

Wang, X. Y., Li, Y. Q., Wang, X. Y., Li, Y. L., Gong, X. W.: Temporal and spatial variations in NDVI and analysis of the driving factors in the desertified areas of northern China from 1998 to 2015, Front. Environ. Sci., 9, 633020. https://doi.org/10.3389/fenvs.2021.633020, 2021.

Watham, T., Padalia, H., Srinet, R., Nandy, S., Verma, P. A., Chauhan, P.: Seasonal dynamics and impact factors of atmospheric $CO_2$ concentration over subtropical forest canopies: observation from eddy covariance tower and OCO-2 satellite in Northwest Himalaya, India. Environ. Monit. Assess., 193, 1-15, https://doi.org/0.1007/s10661-021-08896-4, 2021.

Wilson, K., Goldstein, A., Falge, E., Aubinet. M., Baldocchi, D., Berbigier, P., Bernhofer, C., Ceulemans, R., Dolman, H., Field, C., Grelle, A., Ibrom, A., Law, B.E., Kowalski, A., Meyers, T., Moncrieff, J., Monson, R., Oechel, W., Verma, S. Energy balance closure at FLUXNET sites, Agric. For. Meteorol., 113, 223–243, https://doi.org/10.1016/S0168-1923(02)00109-0, 2002.

Yu, G. R., Zhu, X. J., Fu, Y. L., He, H. L., Wang, Q. F., Wen, X. F., Li, X. R., Zhang, L. M., Zhang, L., Su, W., Li, S. G., Sun, X. M., Zhang, Y. P., Zhang, J. H., Yan, J. H., Wang, H. M., Zhou, G. S., Jia, B. R., Xiang, W. H., Li, Y. N., Zhao, L., Wang, Y. F., Shi, P. L., Chen, S. P., Xin, X. P., Zhao, F. H., Wang, Y. N., Tong, C. L.: Spatial patterns and climate drivers of carbon fluxes in terrestrial ecosystems of China, Glob. Change Biol., 19, 798–810, http://dx.doi.org/10.1111/gcb.12079, 2013.

Yuan, W. P., Liu, S. G., Yu, G. R., Bonnefond, J. M., Chen, J. Q., Davis, K., Desai, A. R., Goldstein, A. H., Gianelle, D., Rossi, F., Suyker, A. E., Verma, S. B.: Global estimates of evapotranspiration and gross primary production based on MODIS and global meteorology data, Remote Sens. Environ., 114, 1416-1431. http://dx.doi.org/10.1016/j.rse.2010.01.022, 2010.

Zhang, C. L.: Photosynthesis and physiological features of different desert species in Horqin Sand land, Minzu University of China, Beijing. Master's Thesis, 2007.

Zhang, Q., Phillips, R. P., Manzoni, S., Scott, R. L., Oishi, A. C., Finzi, A., Daly, E., Vargas, R., Novick, K. A. Changes in photosynthesis and soil moisture drive the

https://doi.org/10.5194/bg-2022-171
Preprint. Discussion started: 19 August 2022
© Author(s) 2022. CC BY 4.0 License.

seasonal soil respiration-temperature hysteresis relationship, Agric. For. Meteorol, 259, 184-195, https://doi.org/10.1016/j.agrformet.2018.05.005, 2018a.

Zhang, R., Zhao, X. Y., Zuo, X. A., Degen, A. A., Li, Y. L., Liu, X. P., Luo, Y. Y., Qu, H., Lian, J., Wang, R. X.: Drought-induced shift from a carbon sink to a carbon source in the grasslands of Inner Mongolia, Catena, 195, https://doi.org/10.1016/j.catena.2020.104845, 2020.

Zhang, R., Zhao, X. Y., Zuo, X. A., Qu, H., Degen, A. A., Luo, Y. Y., Ma, X. J., Chen, M., Liu, L. X., Chen, J. L. Impacts of precipitation on ecosystem carbon fluxes in desert-grasslands in Inner Mongolia, China, JGR. Atmospheres, 124, 1266–1276, https://doi.org/10.1029/2018JD028419, 2019.

Zhang, T., Zhang, Y. J., Xu, M. J., Zhu, J. T., Chen, N., Jiang, Y. B., Huang, K., Zu, J. N., Liu, Y. J., Yu, G. R.: Water availability is more important than temperature in driving the carbon fluxes of an alpine meadow on the Tibetan Plateau, Agric. For. Meteorol, 256–257, 22-31, https://doi.org/10.1016/j.agrformet.2018.02.027, 2018b.

Zhao, H. L., Li, Y. Q., Zhou, R. L.: Effects of desertification on C and N storages in grassland ecosystem on Horqin sandy land (in Chinese), Chin. J. Appl. Ecol., 18, 2412, https://doi.org/10.1360/yc-007-1324, 2007.

Zhou, J., Zhang, Z. Q., Sun, G., Fang, X. R., Zha, T. G., McNulty, S., Chen, J. Q., Jin, Y., Noormets, A.: Response of ecosystem carbon fluxes to drought events in a poplar plantation in Northern China, For. Ecol. Manage., 300, 33-42, https://doi.org/10.1016/j.foreco.2013.01.007, 2013.

Zhou, Y. Y., Li, X. R., Gao, Y. H., He, M. Z., Wang, M. M., Wang, Y. L., Zhao, L. N., Li, Y. F.: Carbon fluxes response of an artificial sand-binding vegetation system to rainfall variation during the growing season in the Tengger Desert. J. Environ. Manage. 266, 110556, https://doi.org/10.1016/j.jenvman.2020.110556, 2020.

Zhu, W. J., Gao, Y., Zhang. H. B., Liu, L. L. Optimization of the land use pattern in Horqin Sandy Land by using the CLUMondo model and Bayesian belief network, Sci. Total Environ., 739, 139929, 10.1016/j.scitotenv.2020.139929, 2020.

Zhu, Z. L., Sun, X. M., Wen, X. F., Zhou, Y. L., Tian, J., Yuan, G. F.: Study on the processing method of nighttime $CO_2$ eddy covariance flux data in China FLUX (in

https://doi.org/10.5194/bg-2022-171
Preprint. Discussion started: 19 August 2022
© Author(s) 2022. CC BY 4.0 License.

Chinese), Sci. China Ser. D., 49, 36–46, https://doi.org/10.1007/s11430-006-8036-5, 2006.

https://doi.org/10.5194/bg-2022-171
Preprint. Discussion started: 19 August 2022
© Author(s) 2022. CC BY 4.0 License.



**Figure captions**

**Fig. 1.** Locations of study area. (a) and (b) are photos of observation site during the growing and dormant seasons, respectively.

**Fig. 2.** (a) Seasonal dynamics of the daily average vapor pressure deficit (*VPD*), (b) photosynthetic photon flux density (*PPFD*), (c) air temperature ($T_a$), (d) the soil temperature ($T_s$) and (e) soil water content (*SWC*) at depths of 10, 30, 50, and 80 cm, and (f) daily precipitation (*PPT*).

**Fig. 3.** Seasonal variability of the daily mean carbon fluxes (*NEE*: net ecosystem $CO_2$ exchange, $R_{eco}$: ecosystem respiration, and *GPP*: gross primary productivity) from 2017 to 2021.

**Fig. 4.** (a-e) Monthly and (f) inter-annual variations of the cumulative carbon fluxes (*NEE*: net ecosystem $CO_2$ exchange, $R_{eco}$: ecosystem respiration, and *GPP*: gross primary productivity) from 2017 to 2021.

**Fig. 5.** Important values of the Random Forest model analysis for the carbon flux (*NEE*: $CO_2$ net ecosystem exchange; $R_{eco}$: ecosystem respiration; *GPP*: gross primary productivity) during the 2017 to 2021 growing seasons. ** and * refer to significance at 0.01 and 0.05 levels, respectively. Variables: *PPFD*: mean photosynthetic photon flux density; $T_a$: mean air temperature; *VPD*: mean vapor pressure deficit; *PPT*: daily total precipitation; $T_s$ and *SWC*: mean soil water content at depths of 10, 30, 50, and 80 cm.

**Fig. 6.** Relationships between seasonal net ecosystem carbon exchange (*NEE*), gross primary productivity (*GPP*), and ecosystem respiration ($R_{eco}$) and the (a) mean photosynthetic photon flux density (*PPFD*) and (b-d) mean soil water contents at depths of 10, 30, and 80 cm ($SWC_{10}$, $SWC_{30}$, and $SWC_{80}$, respectively).

**Fig. 7.** Relationships between monthly net ecosystem carbon exchange (*NEE*) and the main meteorological factors: soil temperature at a depth of 50 cm ($T_{s50}$), mean soil water content at a depth of 30 cm ($SWC_{30}$), vapor-pressure deficit (*VPD*), and photosynthetic photon flux density (*PPFD*).

https://doi.org/10.5194/bg-2022-171
Preprint. Discussion started: 19 August 2022
© Author(s) 2022. CC BY 4.0 License.


**Fig. 8.** Relationships between monthly ecosystem respiration ($R_{eco}$) and the main environmental factors: the soil temperature at a depth of 10 cm ($T_{s10}$), the total precipitation (*PPT*), and the soil water content at a depth of 10 cm ($SWC_{10}$).

**Fig. 9.** Relationships between monthly gross primary productivity (*GPP*) and the main environmental factors: soil temperature at a depth of 10 cm ($T_{s10}$), total precipitation (*PPT*), and soil water content at depths of 80 cm ($SWC_{80}$) and 10 cm ($SWC_{10}$)

https://doi.org/10.5194/bg-2022-171
Preprint. Discussion started: 19 August 2022
© Author(s) 2022. CC BY 4.0 License.


**Fig. 1.**

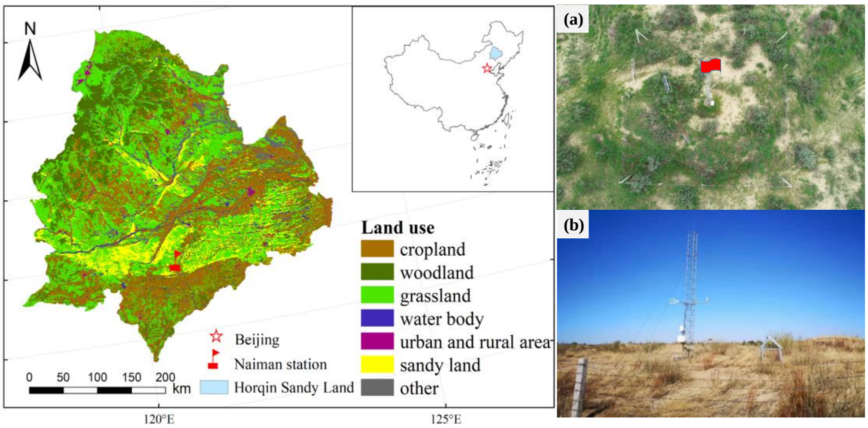


**Fig. 2.**

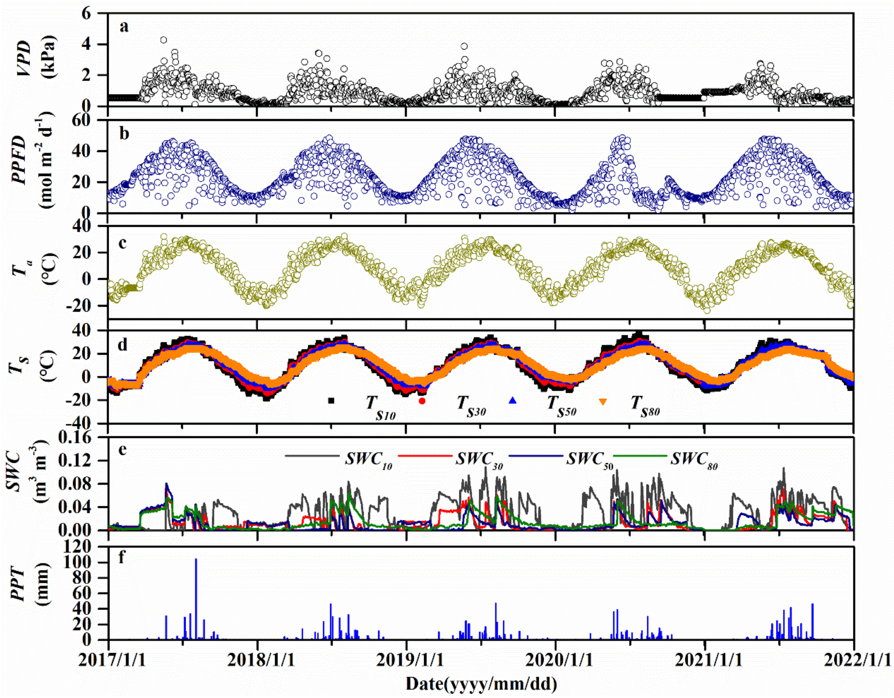

https://doi.org/10.5194/bg-2022-171
Preprint. Discussion started: 19 August 2022
© Author(s) 2022. CC BY 4.0 License.


**Fig. 3.**

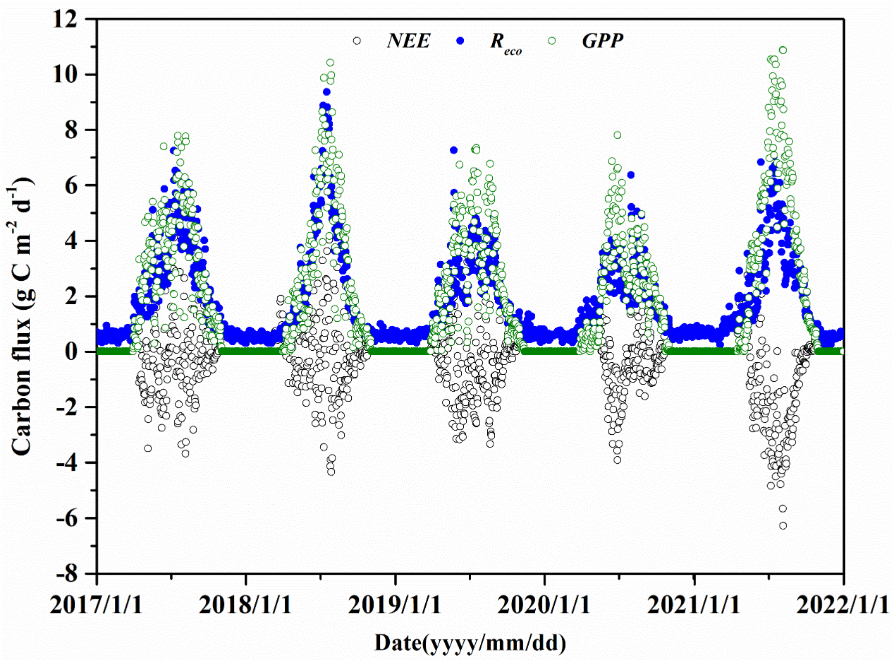


**Fig. 4.**

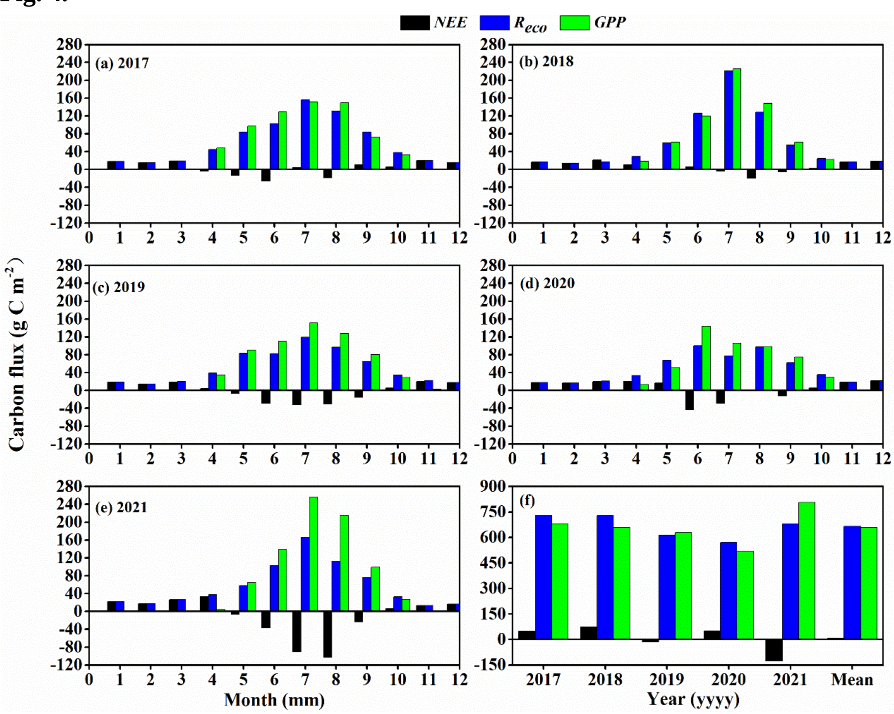

https://doi.org/10.5194/bg-2022-171
Preprint. Discussion started: 19 August 2022
© Author(s) 2022. CC BY 4.0 License.



745 **Fig. 5.**

746 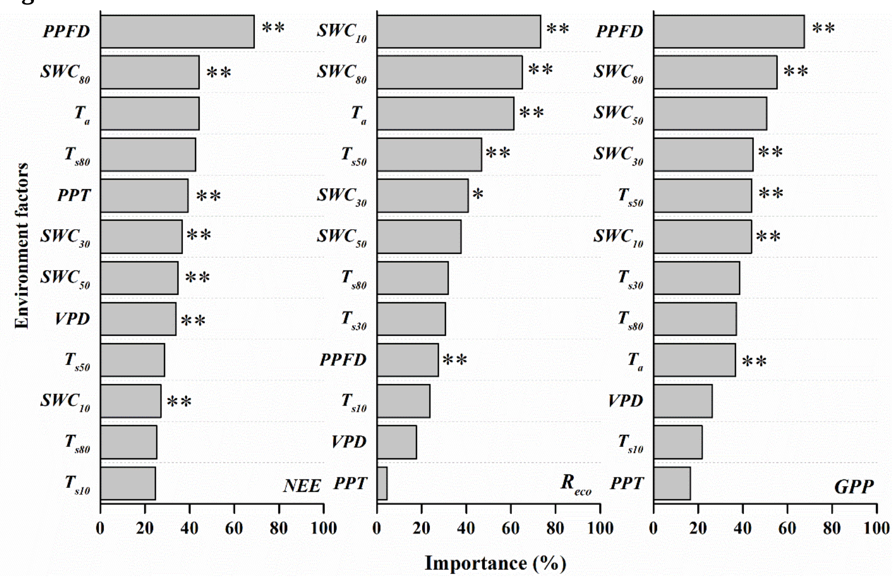


747 **Fig. 6.**

748 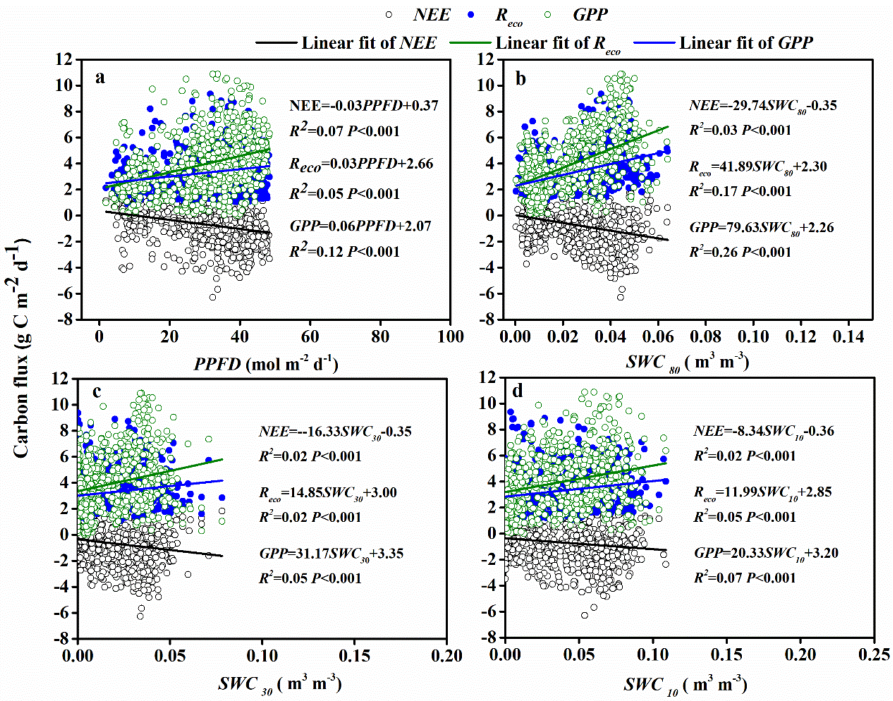

https://doi.org/10.5194/bg-2022-171
Preprint. Discussion started: 19 August 2022
© Author(s) 2022. CC BY 4.0 License.


749 **Fig. 7.**

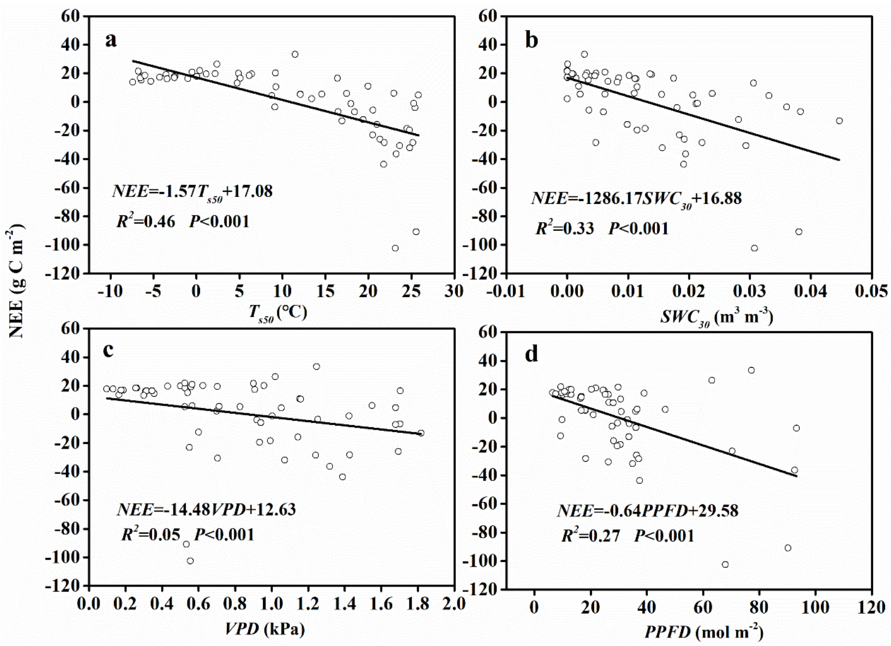


750

751 **Fig. 8.**

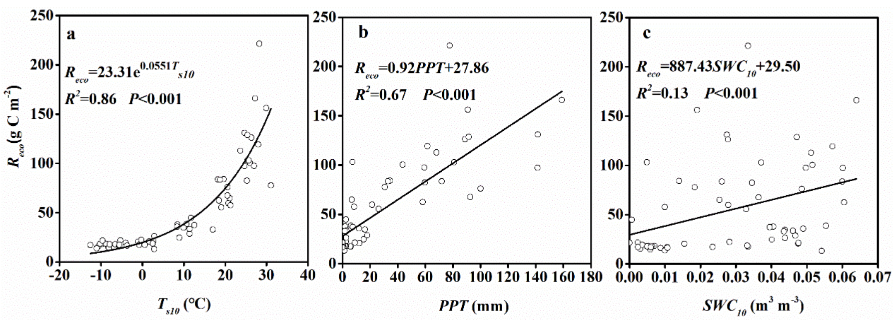


752

https://doi.org/10.5194/bg-2022-171
Preprint. Discussion started: 19 August 2022
© Author(s) 2022. CC BY 4.0 License.


**Fig. 9.**

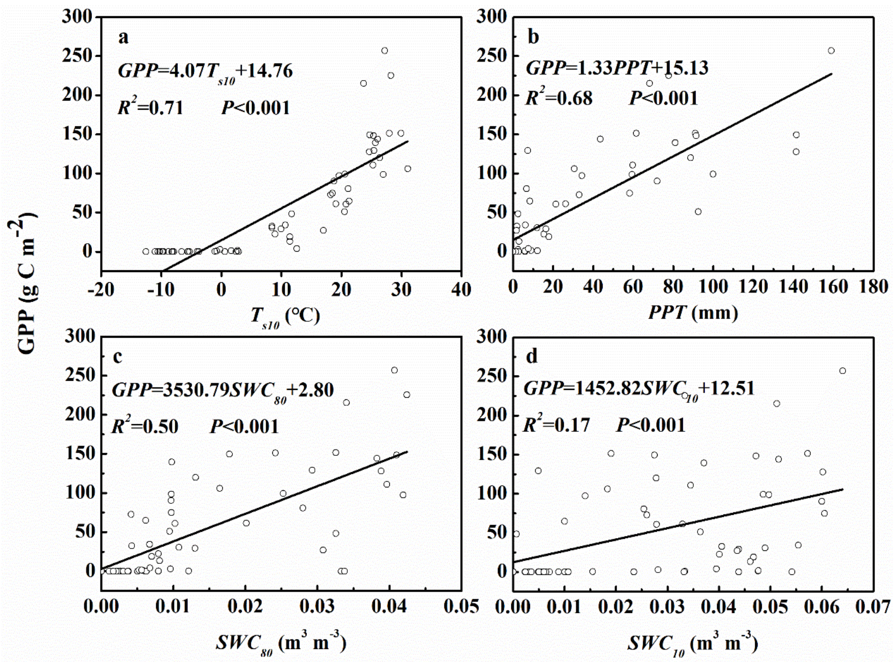

https://doi.org/10.5194/bg-2022-171
Preprint. Discussion started: 19 August 2022
© Author(s) 2022. CC BY 4.0 License.



# Tables

**Table 1** Annual mean meteorological factors from 2017 to 2021 in the semi-fixed sandy ecosystem. Values of a variable labeled the same letter did not differ significantly among the years.

| Year | $T_a$ | *VPD* | *PPFD* | *PPT* | $SWC_{10}$ | $SWC_{30}$ | $SWC_{50}$ | $SWC_{80}$ | $T_{s10}$ | $T_{s30}$ | $T_{s50}$ | $T_{s80}$ |
|---|---|---|---|---|---|---|---|---|---|---|---|---|
| 2017 | 7.90a | 1.00b | 24.00b | 312.80b | 0.014a | 0.015b | 0.016c | 0.016b | 8.79a | 9.16a | 9.68a | 10.28a |
| 2018 | 8.03a | 0.76a | 23.55b | 350.80c | 0.028b | 0.009a | 0.009a | 0.013b | 9.08a | 9.61a | 10.32a | 10.88a |
| 2019 | 8.48a | 0.79a | 23.86b | 382.20d | 0.036c | 0.015b | 0.015b | 0.016b | 9.67a | 10.11a | 10.71a | 11.04a |
| 2020 | 8.26a | 0.79a | 15.44a | 312.00a | 0.034c | 0.009a | 0.009b | 0.011a | 10.83a | 11.02a | 11.11a | 11.20a |
| 2021 | 8.08a | 0.83a | 23.87b | 430.404 | 0.034c | 0.015b | 0.015c | 0.019c | 11.34a | 11.40a | 11.33a | 11.45a |
| Mean | 8.15a | 0.83a | 22.14b | 357.64 | 0.029 | 0.013 | 0.011 | 0.015 | 9.94a | 10.26a | 10.63a | 10.97a |

Note: $T_a$ (°C): air temperature; *VPD* (kPa): vapor pressure deficit; *PPFD* (mol m$^{-2}$ d$^{-1}$): photosynthetic photon flux density; *PPT* (mm): total precipitation; *SWC* (m$^3$ m$^{-3}$) and $T_s$ (°C): soil water content and soil temperature at depths of 10, 30, 50, and 80 cm, respectively.

https://doi.org/10.5194/bg-2022-171
Preprint. Discussion started: 19 August 2022
© Author(s) 2022. CC BY 4.0 License.

**Table 2** The results of multiple stepwise regression analysis of carbon fluxes (*NEE*: net ecosystem exchange; $R_{eco}$: ecosystem respiration; *GPP*: gross primary production) against the potential drivers during the growing season from 2017 to 2021. All regressions were statistically significant at $P < 0.001$.

| Stepwise regression equation | $F$ | $R^2$ |
|---|---|---|
| $NEE = -0.69\ T_{s50}+3.15$ | 51.70 | 0.46 |
| $NEE = -0.53\ T_{s50}+0.33SWC_{30}+3.52$ | 35.10 | 0.54 |
| $NEE = -0.72\ T_{s50}+0.35\ SWC_{30}+0.32\ VPD+4.54$ | 29.57 | 0.59 |
| $NEE = -0.65\ T_{s50}+0.31\ SWC_{30}+0.39\ VPD+0.29\ PPFD+4.43$ | 28.75 | 0.65 |
| $R_{eco} = 0.84\ T_{s10}+4.09$ | 134.62 | 0.70 |
| $R_{eco} = 0.51\ T_{s10}+0.45\ PPT+3.47$ | 113.46 | 0.80 |
| $R_{eco} = 0.61\ T_{s10}+0.50\ PPT-0.22\ SWC_{10}+4.59$ | 91.96 | 0.83 |
| $GPP = 0.34\ T_{s10}+5.71$ | 144.51 | 0.71 |
| $GPP = 0.39\ T_{s10}+0.13\ PPT+4.87$ | 124.75 | 0.81 |
| $GPP = 0.40\ T_{s10}+0.12\ PPT+340.95\ SWC_{80}+5.18$ | 103.03 | 0.84 |
| $GPP=0.42T_{s10}+0.12PPT+333.20SWC_{80}+214.28SWC_{10}+6.82$ | 82.62 | 0.85 |

Note: $T_a$ (°C): air temperature; *VPD* (kPa): vapor pressure deficit; *PPFD* (mol $m^{-2}$ $d^{-1}$): photosynthetic photon flux density; *PPT* (mm): total precipitation; *SWC* ($m^3$ $m^{-3}$) and $T_s$ (°C): soil water content and soil temperature at depths of 10, 30, 50, and 80 cm, respectively.

https://doi.org/10.5194/bg-2022-171
Preprint. Discussion started: 19 August 2022
© Author(s) 2022. CC BY 4.0 License.



**Table 3** The results of correlation analysis (Pearson's *r*) between the inter-annual carbon fluxes (*NEE*: net ecosystem exchange; $R_{eco}$: ecosystem respiration; and *GPP*: gross primary production) and the potential drivers from 2017 to 2021. Significance: *, $P < 0.05$.

| Carbon flux | *PPT* | *VPD* | *PPFD* | $T_a$ | $T_{s10}$ | $T_{s30}$ | $T_{s50}$ | $T_{s80}$ | $SWC_{10}$ | $SWC_{30}$ | $SWC_{50}$ | $SWC_{80}$ |
|---|---|---|---|---|---|---|---|---|---|---|---|---|
| *NEE* | -0.89* | 0.06 | -0.32 | -0.14 | -0.69 | -0.67 | -0.63 | -0.63 | -0.43 | -0.65 | -0.46 | -0.80 |
| $R_{eco}$ | 0.06 | 0.46 | 0.74 | -0.82 | -0.57 | -0.60 | -0.65 | -0.55 | -0.69 | 0.12 | 0.16 | 0.45 |
| *GPP* | 0.74 | 0.26 | 0.76* | -0.45 | 0.15 | 0.11 | 0.05 | 0.12 | -0.13 | 0.58 | 0.45 | 0.93* |

Note: $T_a$ (°C): air temperature; *VPD* (kPa): vapor pressure deficit; *PPFD* (mol m$^{-2}$ d$^{-1}$): photosynthetic photon flux density; *PPT* (mm): total precipitation; *SWC* (m$^3$ m$^{-3}$) and $T_s$ (°C): soil water content and soil temperature at depths of 10, 30, 50, and 80 cm, respectively.